

3 TRANSMISSION OF CONCENTRATED STRESSES
TO A THIN WALLED SHELL 5

6 V. I. Feodos'yev and S. M. Chernyakov 9

Translation of 5'0 peredache sosredotochennykh sil na tonko-
stennuyu obolochku. 6
Inzhenernyy Zhurnal, Mekhanika Tverdogo Tela, No. 6, pp. 57-
63, 1966.

FACILITY FORM 802

N67-27534

(ACCESSION NUMBER)

1012

(PAGES)

(NASA CR OR TMX OR AD NUMBER)

(THRU)

(CODE)

(CATEGORY)

GPO PRICE \$ _____

CFSTI PRICE(S) \$ _____

Hard copy (HC) 8.00Microfiche (MF) 165

853 July 65

1. See pg 11

NATIONAL AERONAUTICS AND SPACE ADMINISTRATION
Washington, D. C. 20546

9 March 1967 10

TRANSMISSION OF CONCENTRATED STRESSES
TO A THIN WALLED SHELL

V. I. Feodos'yev and S. M. Chernyakov

ABSTRACT. The transmission of stresses to a thin-walled shell over a limited contact region is studied. It is shown that when the shell is completely free from radial stresses on the side of the insert, but clamping is retained, the values of the radial force are decreased by approximately a factor of two.

The force diagrams for many structures include the transmission of stresses to a thin-walled shell over a limited contact region.

/57*

Naturally, in this case it is necessary to take measures to strengthen the structure. The placement of ribs or longerons is not always possible, and it is frequently necessary to satisfy the requirements only by local strengthening of the shell, which makes possible more uniform distribution of stresses.

The question arises regarding the establishment of an approach to the design of such joints.

Many investigations have been conducted, the results of which give us a clear concept of the laws governing the distribution of stresses in the zone of action of the concentrated load applied to a shell. These investigations have been principally concerned with the determination of the local stresses in the region of apertures or rigid inserts into the body of the shell.

However, for plastic materials the fatigue life for the structure under localized loading was generally not determined. The stressed state is not the criterion by which one can design such structural joints. Even at relatively large loads and significant local plastic deformations the structure does not lose its load-carrying properties and completely satisfies the requirements.

This work is concerned with the solution of an example from a class of such problems, obtained in the course of designing a real structure. This solution shows the recommended approach to the problem and the method of analysis.

Let us consider a thin walled spherical shell, subjected to stress by a uniform internal pressure p and radial force P at the center of a circular

*Numbers given in the margin indicate pagination in original foreign text.

flange (Figure 1a). The flange (Figure 1b) consists of a rigid core with radius r_0 and a section $r_0 < r < r_1$. The variable thickness of this latter section promotes more uniform distribution of forces. Both the flange and the shell are constructed of aluminum-magnesium alloys. The stress diagram for the alloy is shown in Figure 2.

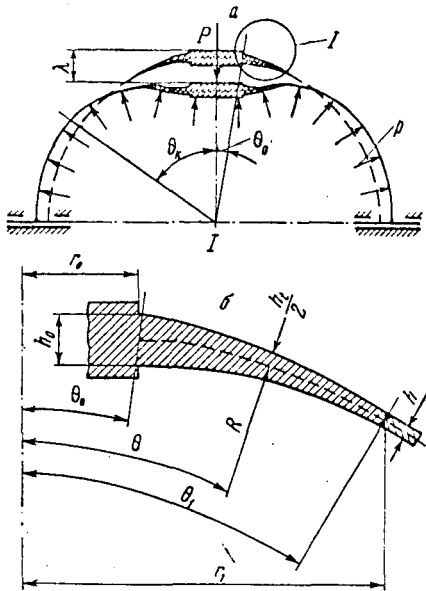


Figure 1

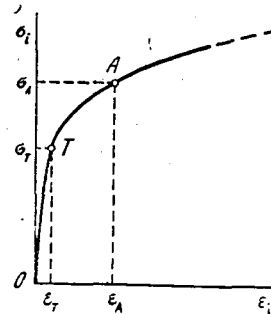


Figure 2

The occurrence of plastic deformation in the shell does not produce qualitative changes in the behavior of the system. Therefore, the evaluation of the stressed state of the shell for design purposes is not as valuable as is frequently ascribed to this operation. Let us attempt to view this problem from a different standpoint.

The "force displacement" diagram for the shell had the shape of one of the curves which are shown in Figure 3. Depending on the geometric relationships the shape of the diagram may change. In some cases the curve (1) has a maximum, while in others it (2,3) has a monotonic character but at some value of force the rate of increase of the displacement is rapidly accelerated. Due to the high plastic properties the shell is not ruptured, and its shape may vary without the disruption within extremely broad limits. The $P-\lambda$ diagram is a characteristic of the structure. It describes the behavior of the structure from the beginning of loading to some limit. The designer who makes use of such a diagram can decide where he must stop and to what limit a given structure can be loaded. Such an approach is completely analogous to the design for permissible stresses. In the latter case, however, the stress is determined not from the shape of the structural characteristics, but from the test diagram of the material.

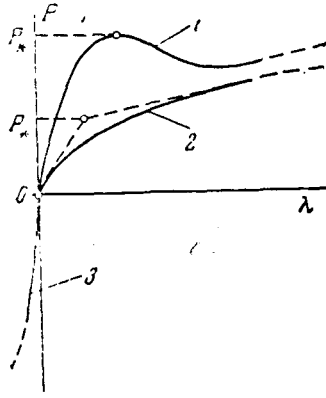


Figure 3

In the proposed approach one may introduce a reserve coefficient, P , for which it is necessary to decide a priori on a certain characteristic limiting point on the $P-\lambda$ curve. It is generally convenient to take for such a point either the maximum point, or a point which corresponds to a rapid increase of displacement.

Such an approach naturally permits one if necessary, to take into consideration the magnitude of stresses which occur in the shell in the course of loading. The problem of constructing $P-\lambda$ diagrams is naturally more compli-

cated in the case of large displacements and plastic deformations. These difficulties can be overcome by means of the step method [1]. Here, however, in contrast to the work described in [1], the independent parameter is the displacement of a point, at which the applied stress is taken as the independent parameter rather than the time, t .

1. Let w and u denote the displacements of points of the inner surface of the shell in a vertical direction downward (along the direction of the force P) and along the horizontal plane respectively. The angle of rotation of the normal is denoted through ϑ . At a distance $z = \eta h$ from the inner surface of the shell we shall have

$$\varepsilon_{1z} = \varepsilon_1 + \eta h \kappa_1 \frac{h_t}{h}, \quad \varepsilon_{2z} = \varepsilon_2 + \eta h \kappa_2 \frac{h_t}{h} \quad (1.1)$$

where ε_1 and ε_2 are deformations in the inner surface; $h \kappa_1$ and $h \kappa_2$ are dimensionless changes of curvature; h is the thickness of the shell and h_t is the variable thickness of the flange, for which the equation describing changes is taken to be linear (Figure 1b).

$$h_t = h + (h_0 - h) \frac{\theta_1 - \theta}{\theta_1 - \theta_0} \quad (1.2)$$

From the geometric relationship it follows that

$$\begin{aligned} \varepsilon_1 &= \frac{h}{R} [U' \cos(\theta + \vartheta) + W' \sin(\theta + \vartheta)] + \cos \vartheta - 1, \quad \varepsilon_2 = \frac{h}{R} \frac{U}{\sin \theta} \\ h \kappa_1 &= \frac{h^2}{R^2} [(W'' - 2U') \cos(\theta + \vartheta) - \\ &\quad - (2W' + U'') \sin(\theta + \vartheta)] + \frac{h}{R} (1 - \cos \vartheta) \\ h \kappa_2 &= \frac{h}{R} \left[\frac{\sin(\theta + \vartheta)}{\sin \theta} - 1 - \frac{h}{R} \frac{U}{\sin \theta} \right] \end{aligned} \quad (1.3)$$

$$\tan \vartheta = \frac{W' \cos \theta - U' \sin \theta}{R/h + U' \cos \theta + W' \sin \theta} \quad \left(W = \frac{w}{h}, \quad U = \frac{u}{h}, \quad ()' = \frac{d()}{d\theta} \right) \quad (1.3)$$

cont'd

The intensity of the deformed state ε_i in points, located at a distance 159 z from the inner surface shall be

$$\varepsilon_i = \frac{2}{\sqrt{3}} \sqrt{\varepsilon_{1z}^2 + \varepsilon_{1z}\varepsilon_{2z} + \varepsilon_{2z}^2} \quad (1.4)$$

Let us assume for the elastic zone, just as for the plastic zone, that $\mu = 0.5$, and let us approximate the stretching -- compression diagram by the following relationship:

$$\frac{\sigma_i}{E} = \varepsilon_i \quad (0 \leq \varepsilon_i \leq \varepsilon_r), \quad \frac{\sigma_i}{E} = A + B \sqrt{C + D\varepsilon_i} \quad (\varepsilon_i \geq \varepsilon_r) \quad (1.5)$$

where A, B, C and D are dimensionless constants, selected from the shape of the diagram (along the coordinates of points A and T in Figure 2).

Subsequently we shall not take into account the possibility of the occurrence of the relief zones, i.e., the material is viewed as nonlinearly elastic.

2. Let

$$W = A_0 W_0 + A_2 W_2 + A_4 W_4 + W_p \quad (2.1)$$

$$U = (A_0 + B_0) U_0 + B_1 U_1 + B_3 U_3 + B_5 U_5 + U_p$$

Here $W_0, W_2, \dots; U_0, U_1, \dots$ are some specially selected functions of the angle θ , and $A_0, A_2, \dots; B_0, B_1, \dots$ are parameters which vary in the course of change of the load.

of the parameters

From the second and the last expressions in equation (1.3), independent of $A_0, A_2, \dots; B_0, B_1, \dots$, we have

$$U = 0, \quad W' \cos \theta_0 - U' \sin \theta_0 = 0 \quad (\text{when } \theta = \theta_0) \quad (2.2)$$

At sufficiently large angle θ functions W and U must assume the form which is characteristic of the momentless state of the shell, loaded by a force at the pole and by the internal pressure.

The construction of a system of functions $W_0, W_2, \dots; U_0, U_1, \dots$, which would satisfy these conditions, presents some difficulties.

Experience shows that the shape of the indentation changes significantly with increase of sag and penetration of the plastic deformation region. It

remains, however, axially symmetrical. In choosing functions it is necessary to take into account the parameters of the "feather", i.e., the transition section with variable thickness of the wall h_t . It is the dimensions of this very section which determine how effective the joint is and how smoothly the stresses are redistributed.

The principal functions in the expression (2.1) are W_0 and U_0 . They are determined by a linear solution of the loading force P without the pressure p for the shell.

The determination of these functions with modern computer technology does not present any great difficulties. For the axially symmetrical shell with variable wall thickness Meisner equations are integrated numerically.

The integration is carried from $\theta = \theta_0$ to some randomly taken value $\theta = \theta_k$, where the shape of the indentation, on the basis of continuity conditions, merges with the momentless state zone. With two boundary conditions at $\theta = \theta_0$ the solution is reduced to the successive process of search for two other parameters, the magnitude of which would insure the adherence to the assigned conditions when $\theta = \theta_k$. It is desirable to take the angle θ_k as small as possible, in order to shorten the calculation time. At the same time it must be sufficiently large in order to permit joining of the two parts of the shell when $\theta = \theta_k$ on the basis of simplified equations of the edge effect. The choice of θ_k is conducted on the basis of an approximate evaluation of the rate of attenuation of the moment state for the assigned value of h/R . If the increase of θ_k does not lead to change of functions W_0 and U_0 then the angle θ_k was taken sufficiently large. If functions W_0 and U_0 change significantly then the angle θ_k should be enlarged. This operation may be directly programmed into a computer, but it is not mandatory. When the approximation has been made and the shape of the elastic surface has been found, the functions W_0 and U_0 and their derivatives are normalized. Their scales are at the same time changed in order for W_0 to be equal to unity at $\theta = \theta_0$. Therefore, the magnitude of force P , entering the Meisner equation in the course of construction of these functions could be taken randomly. /60

Using the same subprogram the second integration of the Meisner equation is conducted, but in this case at $P = 0$ and some value of p , which is introduced into the calculation in a dimensionless form. Thus, functions W_p and U_p are found. The determined functions W_0 , U_0 , W_p and U_p , as well as their first and second derivatives are introduced into the operational memory of the computer. For this purpose a number of points are taken within the

limits of indentation, i.e., within the limits of angle $\theta_k - \theta_0$, for each of which functions and derivatives are written. In our calculations 64 such points were taken.

The forms of functions W_0 , U_0 , W_p and U_p are shown in Figure 4.

As an illustration we give some values of these functions for different values of angle θ for the shell with a rigid flange (without a feathered edge) and parameters $R = 280$ mm, $h = 1.3$ mm, $\theta_0 = 4^\circ 30'$ when $p = 0$ (W_0 , U_0) and $p = 3.3$ kg/cm² (W_p , U_p):

$\theta = 4^\circ 30'$	$7^\circ 15'$	10°	$12^\circ 45'$	$18^\circ 15'$	$29^\circ 15'$	$45^\circ 45'$
$W_0 = 1.0$	0.5576	0.1388	0.0060	0.0062	0.0080	0.0007
$U_0 = 0$	0.0259	0.0662	0.0743	0.0507	0.0304	0.0207
$W_p = -0.0322$	0.0416	-0.0505	-0.0528	-0.0518	-0.0469	-0.0374
$U_p = 0$	0.0047	0.0089	0.0121	0.0170	0.0264	0.0387

The auxiliary functions W_2 , W_4 , U_1 , U_3 and U_5 in the expression (2.1) were taken in the form

$$W_n = U_n = (\theta - \theta_0)^n e^{-k(\theta - \theta_0)}.$$

The quantity k was not varied although it shall be shown later, that this could have been done.

As the first approximation we take

$$k = \sqrt[4]{R/h} \sqrt[3]{3(1-\mu^2)}.$$

Subsequently satisfactory agreement of calculations was found with the preliminary experiments; therefore the previously taken value for k was retained.

Let us now consider the expressions for W and U (2.1) as a whole.

Since $W_0 = 1$ and $W_2 = W_4 = 0$ when $\theta = \theta_0$, the parameter A_0 provides the displacement $\lambda = A_0 h$ under the in-

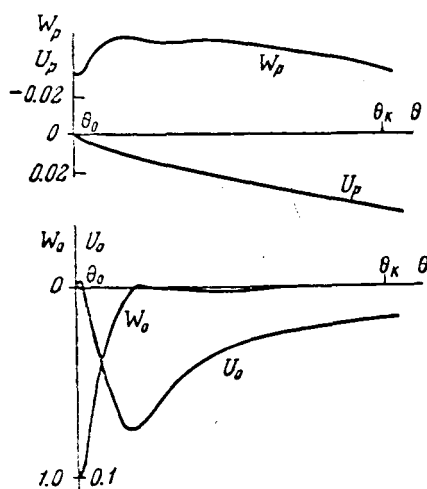


Figure 4

fluence of the pressure P for the shell, pressurized beforehand with pressure p . All of the functions U_0, U_1, \dots become zero when $\theta = \theta_0$. Consequently, the condition $U = 0$ on the inner surface is fulfilled at any values of parameters A_0, B_0, B_1, \dots

The condition (2.2) is fulfilled if

$$B_1 = -B_0 (U_0')_{(\theta=\theta_0)} \quad (2.3)$$

Thus, parameters B_0 and B_1 are interrelated.

3. The expression for the total potential energy of the system has the following form:

$$\mathcal{D} = \int_{\Omega} \left(\int_0^{\epsilon_i} \sigma_i d\epsilon_i \right) d\Omega + pV - PA_0 h \quad \left(\mathcal{D}_0 = \frac{\mathcal{D}}{2\pi ER^2 h} \right) \quad (3.1)$$

Here Ω is the volume of the deformed section of the shell, V is the /61 volume of the inner region of the vessel and \mathcal{D}_0 is the energy in a dimensionless form. The expression (3.1) is transformed finally to the form

$$\mathcal{D} = \mathcal{D}(A_0, A_2, A_4, B_0, B_3, B_5, p, P) \quad (3.2)$$

The parameter B_1 is not included into this expression, since it is related to B_0 by the equation (2.3). In the equilibrium position

$$\delta \mathcal{D} = 0 \quad (3.3)$$

The equality (3.3) is fulfilled with simultaneous conversion of partial derivatives to zero

$$\frac{\partial \mathcal{D}}{\partial (\)_n} = \int_{\Omega} \sigma_i \frac{\partial \epsilon_i}{\partial (\)_n} d\Omega + p \frac{\partial V}{\partial (\)_n} - P \frac{\partial \lambda}{\partial (\)_n}$$

which after transformation may be written in the dimensionless form

$$F_n = \frac{\partial \mathcal{D}_0}{\partial (\)_n} = \int_{\theta_0}^{\pi} \int_{-1}^1 \frac{\sigma_i}{E} \frac{\partial \epsilon_i}{\partial (\)_n} \sin \theta d\eta d\theta - \frac{h}{R} P_0 \frac{\partial A_0}{\partial (\)_n} + \frac{p_0}{2\pi R^3} \frac{\partial V}{\partial (\)_n} \quad (n=0, 1, \dots, 5) \quad (3.4)$$

$$P_0 = \frac{P}{2\pi ERh}, \quad p_0 = \frac{pR}{Eh}$$

The notation $\partial/\partial (\)_n$ designates differentiations with respect to one of the variable parameters. Let

$$F_0 = \frac{\partial \mathcal{D}_0}{\partial A_0}, \quad F_1 = \frac{\partial \mathcal{D}_0}{\partial A_2}, \quad F_2 = \frac{\partial \mathcal{D}_0}{\partial A_4}, \quad F_3 = \frac{\partial \mathcal{D}_0}{\partial B_0}, \quad F_4 = \frac{\partial \mathcal{D}_0}{\partial B_3}, \quad F_5 = \frac{\partial \mathcal{D}_0}{\partial B_5}$$

Subsequently, we go stepwise, setting all parameters $A_0, A_2, \dots, B_0, \dots$ prior to the first step equal to zero.

The sequence of operations is reduced to the calculation of quantities $\epsilon_1, \epsilon_2, h\kappa_1, h\kappa_2, \tan \vartheta, \epsilon_{1z}, \epsilon_{2z}$ and $\epsilon_i, \sigma_i/E$ according to equations (1.1) - (1.5) and knowing A_0, A_2, \dots from the previous step. For this the values of functions U_n, W_n and their derivatives are used, recorded in the operative memory of the computer. From the same functions the volume of the inner region V bounded by the deformed cell is determined.

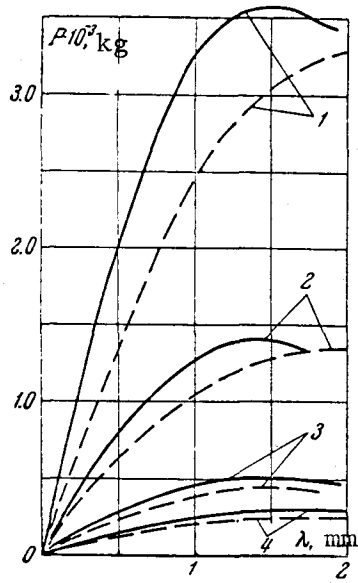


Figure 5

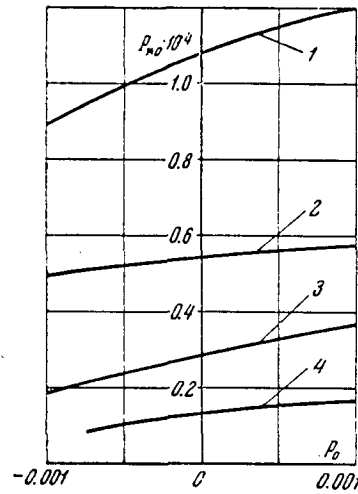


Figure 6

Since during flexure of the shell the stress over the thickness changes, the calculations of $\epsilon_{1z}, \epsilon_{2z}, \epsilon_i$ and σ_i/E must be conducted for a number of points, located along the normal. In the considered example, the thickness was broken up into ten sections. Consequently, 11 points were obtained.

The main characteristic of the program is the cyclic nature of its construction, which is necessary for the determination of partial derivatives. Each of the varied parameters is in turn increased by a quantity δ .

In order to find the quantity F_n , we calculate ϵ_i for parameters $A_0, A_2, \dots, B_0, \dots$ of the previous step. Following this, for example, the quantity A_n with all other parameters being the same is increased by δ , and calculations are repeated. The difference thus found between the quantity ϵ_i , divided by δ , gives $\partial \epsilon_i / \partial A_n$. By carrying out the integration over the thickness and over the angle θ we find F_n (3.4).

For the determination of the coefficients in the system (4.1) it is necessary to have derivatives of F_n , which are obtained by the same method.

Therefore, the program for the determination of the coefficient in the system (4.1) is constructed by the "cycle in the cycle" principle, as a result of which a matrix a_{ij} is obtained.

By assigning the step $\Delta A_0 = \Delta \lambda / h$, we solve the system (4.1) and find the increases $\Delta A_2, \Delta A_4, \Delta B_0, \dots$, which are added to the previous values of A_2, A_4, B_0, \dots , after which we proceed with the next step. The parameter of the pressure P_0 is determined for each step from the expression (3.5). Thus, in the dimensionless form a diagram $P_0 = f(A_0)$ is constructed. Having such a diagram one may solve the questions regarding the suitability of the proposed structure.

Many calculations have shown that the limiting state, corresponding to the maximum pressure P , is achieved when the indentation λ is of the order of 1 - 2 thicknesses of the shell, i.e. when $A_0 \approx 1 - 2$. The step ΔA_0 , which insures more than sufficient technical accuracy, may be taken of the order of 0.05 - 0.1. Therefore, the computer time which is necessary for the construction of one diagram, is relatively small (of the order of 20 - 30 minutes). Thus, in a few hours of work one can observe the effect of the principal structural parameters: angle θ_0 , angle θ_1 and the thickness of the feathered edge of the rib. The effect of the dimensions of the taper of the rib on the shape of the diagram is quite significant.

Figure 5 shows a comparison of the calculated curves (solid lines) with the experimental curves (broken lines) for shells with circular flange without the taper for the case when $p = 0$. Each pair of curves refers to one of the shells with the following values of parameters h and θ_0 (radius $R = 280$ mm is the same for all shells): 1 (2.6 mm, $10^\circ 54'$), 2 (2 mm, $7^\circ 10'$), 3 (1.3 mm, $4^\circ 30'$), 4 (1.7 mm, $1^\circ 50'$). The existing discrepancies are relatively small and quite permissible from the practical standpoint.

The carrying capacity of shells can be conveniently classified by means of the parameter $h\theta_0^2/R$. For the above considered shells 1, 2, 3, and 4 with parameter $h\theta_0^2/R = 3.4 \cdot 10^{-4}, 1.2 \cdot 10^{-4}, 0.28 \cdot 10^{-4}, 0.062 \cdot 10^{-4}$. Figure 4 shows the limiting loads as a function of pressure and the dimensions of the shell.

Figure 7 for the shell with parameter $h\theta_0^2/R = 0.28 \cdot 10^{-4}$ shows the effect of the dimensions of the flange with the taper on the quantity P_{*0} when $p_0 = 0$.

The principal error which arises in the calculations of such structure is associated with deviations of the conditions along the inner periphery from the assumed rigid joint. The welded seam and the insert itself have a certain pliancy. This leads to partial weakening of the applied bond in the most strongly

strongly deformed zone of the shell and has a significant effect on the $P = f(\lambda)$.

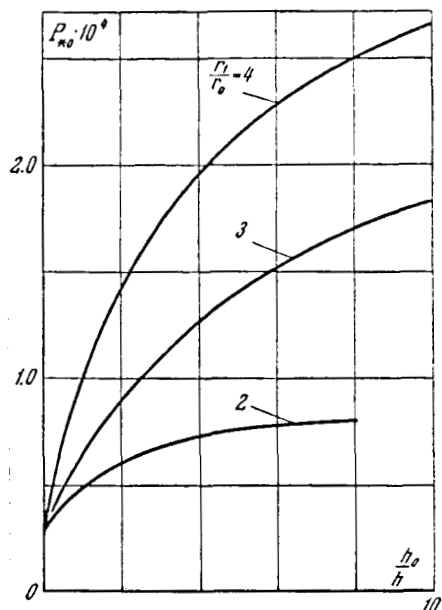


Figure 7

The conducted calculations have shown that in the limiting case when the shell is completely free from radial stresses on the side of the insert, but when clamping is preserved, the values of corrected P are lowered by approximately a factor of two.

The effect of the magnitude of the Poisson coefficient was determined. The change from the value $\mu = 0.5$ to $\mu = 0.3$ did not have any significant effect on the shape of the $P = f(\lambda)$ diagram.

REFERENCES

1. Feodos'yev, V. I.: A Method for Solving Nonlinear Stability Problems in Deformable Systems, PMM (Applied Mathematics and Mechanics), 27, No. 2, (1963).

Translation prepared for the National Aeronautics and Space Administration by
INTERNATIONAL INFORMATION INCORPORATED, 2101 Walnut St., Philadelphia, Pa. 319103
Contract No. NASw-1499.

25 29